Biomass-mapping of alpine grassland with APEX imaging spectrometry data

Maja Rapp
UNIGIS MSc, Universität Salzburg / Schweizerischer Nationalpark
Schloss Planta Wildenberg
7530 Zernez
maja.rapp@nationalpark.ch

Abstract — Today remote sensing is a standard technique for mapping land cover in high spatial resolution over large areas. Not only land cover but also the quality and quantity of vegetation can be classified by the analysis of hyperspectral data. In the Swiss National Park (SNP) we use data from the Airborne Prism Experiment (APEX) imaging spectrometer to expand the possibilities of vegetation analysis in alpine territories. The high spectral and spatial resolution of APEX data allows the correlation of the measured reflection with ground truth data. We tested a standard Normalized Differenced Vegetation Index (NDVI) and an optimized simple ratio index (SRI) with selected bands to model the biomass content of the alpine grassland of one particular valley in the SNP, the Val Trupchun. The correlation between biomass *insitu* measurements and SRIs was non-linear, most likely due to sensor saturation. Our optimal SRI improved the model quality compared to the NDVI model. All computed models underestimated high biomass values above 600 g/m^2. The model accuracy of 57% was good considering the challenging terrain. However, several factors showed that the model was relatively unstable due to parameter input settings and external factors. Differences in APEX data between strips induced an important effect, due to different illumination/view angles. The variability analysis investigating the sample plot location demonstrated that small-scale geometrical shifts were insignificant compared to the overall model accuracy. The biomass prediction map showed plausible values for the grassland with high concentrations around former alps. High biomass sources were linked to former anthropogenic land use, dominant vegetation structure and to preferred ungulate habitat today. The high-resolution map is now a useful basis for future research in the SNP to investigate forage amount and analyse ungulate habitat pattern in Val Trupchun. This a welcoming issue for ungulate research, which is an important research area of the SNP.

Keywords — imaging spectrometry, hyperspectral data, biomass modeling, vegetation indices

1 INTRODUCTION

Imaging spectrometry or imaging spectroscopy is a remote sensing technique recording the earth's surface by a hyperspectral sensor. With increased number of spectral bands and increased spatial resolution the technique allows today not only the mapping of land cover types but also the mapping of vegetation quality and quantity.

An imaging spectroscometer samples contiguously in the optical part of the electromagnetic spectrum using dozens to hundreds of narrow spectral bands. For each image pixel, the sensor acquires the reflectance of the earth's surface from the ultraviolet through the visible to the near- and mid-infrared (i.e. 250 - 2500 nm) part of the electromagnetic spectrum at a high spatial resolution.

In Fig. 1 a schematic of the function of an imaging spectrometer is illustrated.

Analysing the vegetation using remotely sensed data requires knowledge of the biochemical, structural and functional vegetation characteristics and its optical properties. Water, pigments, nutrients and carbon are each expressed in the reflected optical spectrum from 400 nm to 2500 nm, with often overlapping, but spectrally distinct, reflectance behaviours. The absorption characteristics of these compounds determine the optical properties, which as a result are then visible in e.g. the reflectance spectra. These known signatures allow scientists to combine reflectance measurements at different wavelengths to enhance specific vegetation characteristics[1]. Vegetation indices (VIs) have been widely adopted for studying vegetation

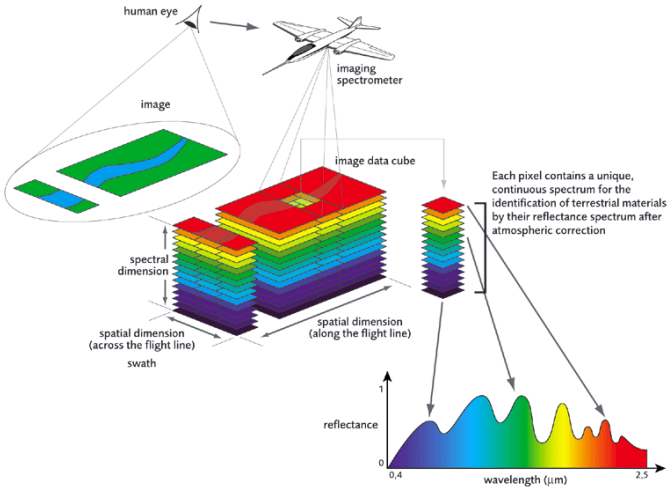

Fig. 1: Working Schematic of a imaging spectrometer (Image: www.apex-esa.org, last accessed 20.03.2013)

cover, chlorophyll content or quantifying other vegetation properties. As different materials have characteristic spectra with maxima or minima at particular wavelengths, there is often no need for complex physical models to determine key biophysical parameters. VIs based on empirical or semi-empirical models are new variables generated by mathematical combination of two or more of the original spectral bands chosen in such a way that the new indices are related to the biophysical parameters of interest. A variety of VIs have been published so far. Well-known and simply applicable VIs are the Normal-

[1] From ENVI User's Guide: Vegetation Indices. http://geol.hu/data/online_help/Understanding_Vegetation_and_Its_Reflectance_Properties.html, last accessed on 20.03.2013.

ised Differenced Vegetation Index (NDVI, Rouse et al., 1974; Tucker, 1979) and the Simple Ratio Index (SRI, Birth and McVey, 1968; Rouse et al., 1974; Tucker, 1979). These indices are typically used for modelling the healthy green vegetation or quantifying the photosynthetic capacity of plant canopies. With the advent of imaging spectroscopy and the availability of the large amount of narrow spectral bands, vegetation indices can be individually designed for a specific vegetation property and a specific territory. By correlating the results of the VIs with on site field data, the optimal VI is chosen to model the desired vegetation property. The advantage of the index implementing two to many bands is to minimize the sensitivity to irradiance, illumination and to other factors such as variation in atmospheric transmission. The disadvantage of empirical models and VIs is that the structural property of the vegetation can't be modelled. Especially for dense canopies (high biomass) the VI have its limitations due to saturation.

Studies using hyperspectral data to estimate biomass by relating field data to vegetation indices have been carried out in several studies. (Mutanga & Skidmore, 2004; Rahman & Gamon, 2004; Mirik et al., 2005; Tarr et al., 2005; Beeri et al., 2007; Cho et al., 2007; Psomas et al., 2009). These studies show the complexity of the spectral response of mixed grasslands, especially in the presence of a high fraction of NPV and exposed soil (Beeri et al., 2007; He et al., 2006; Boschetti et al., 2007), grazing impact (Numata et al. 2007), canopy architecture complexity due to mixed species composition and phenology (Cho et al., 2007; Numata et al. 2008), and sensor saturation occurring at high biomass concentration (Mutanga & Skidomre 2004). Using grass (*Cenchrus ciliaris*) grown in the greenhouse, Mutanga & Skidmore (2004) showed that narrow-band NDVI computed from 740 and 755 nm (both in the far RED) solved the saturation problem when estimating grass biomass at high canopy cover.

The Swiss National Park (SNP) was mapped by APEX (Airborne Prism Experiment) for the first time in June 2010. Land cover mapping and monitoring of landscape dynamics are essential for the management of protected areas. Since ungulate research plays an important role in the SNP, the application possibilities of the APEX data are of great interest. Until now, vegetation mapping has been based on the interpretation of single plots and visual observations, which enables only limited interpolations over large areas. Since 1917, the vegetation has been monitored on more than 150 permanent plots (Braun-Blanquet et al., 1931). In 1968 an analogue vegetation map of part of the SNP was produced in cartography work by Trepp/Campell at a scale of 1:10'000 (Trepp & Campbell, 1968). In 1992, Zoller published a vegetation map of the entire SNP (Zoller, 1992). It was based on observation plots and field trips, and mapped at a 1:50'000 scale. An interpretation of colour infra-red aerial images was conducted over the whole territory of the SNP as part of the project Alpine Habitat Diversity (HABITALP[2]) in 2006. The HABITALP project has been the first study with a standardized method to classify vegetation types area-wide from aerial images. With APEX not only a classification of habitat types is possible, but also pixel-based modelling of vegetation composition at a scale of 2 x 2 meters.

Despite the 100 years of protection, traces from the former land use can still be found on subalpine and alpine grassland. Cattle and sheep grazed the territory of the SNP for several centuries until 1914 (Parolini, 1995). As a result, tall-herb communities dependent on nutrient enrichment from the excreta of cattle or sheep can still be found on several former pastures in the SNP (Braun-Blanquet, 1931; Braun-Blanquet et al., 1954; Achermann et al., 2000).

2 OBJECTIVE

The aim of this MSc thesis is to generate a biomass map of the grassland of one particular valley of the SNP (Val Trupchun) with APEX imaging spectrometry data from June 2010. A semi-empirical method is implemented in the modelling process. First, a standard normalized-differenced-vegetation-index (NDVI) is calculated and compared with *insitu* biomass samples. To achieve a better model, a large number of simple ratio vegetation indices (SRI) are developed from the hyperspectral data and regressed against the ground truth data. Model validation is carried out by independent sample plots. The best model is taken to predict the grassland biomass in Val Trupchun. The produced biomass map is analysed for accuracy and plausibility relating to the former land use of the Val Trupchun.

3 METHODOLOGY

3.1 The study area

The Swiss National Park (SNP) was founded in 1914 as a strict nature reserve and is the oldest national park in the Alps. The park is situated in the canton of Graubünden covering an area of 170 km^2, which is the largest protected area in Switzerland. The national park is classified as a category I nature reserve (highest protection level - strict nature reserve /wilderness area) with the IUCN (International Union for the Conservation of Nature). The territory encompasses an alpine landscape extending over altitudes between about 1400 to 3200 meters above sea level (asl.) with a rich flora and fauna. The study site Val Trupchun is one particular valley of the park, located in the north (46°40'N, 10°15'E) within the territory of the Municipality of S-chanf.

3.2 The APEX instrument

The Airborne Prism Experiment (APEX) is a airborne imaging spectrometer developed under the scientific lead of a Swiss-Belgian collaboration between the Remote Sensing Laboratories (RSL, University of Zurich (CH)) and the Flemish Institute for Technological Research VITO (B) on behalf of the European Space Agency (ESA) PRODEX programme.

APEX is built as a pushbroom dispersive imaging spectrometer recording more than 330 spectral bands contiguously. The instrument specifications can be found in Tab. 1. The APEX mission for the SNP acquired 186 km^2 at a 2x2 m spatial resolution determined by the sensor's instantaneous field of view (IFOV) in combination with a flight height of 4400 - 5400 m asl. 1000 pixels were recorded across-track with a data rate of 0.42 GBytes/km per flight path. The spectral configuration was set to 312 spectral bands to be acquired simultaneously. We used 301 bands for analysis, after some bands had to be removed due to noise. The sensor was installed on a Research Aircraft Dornier DO-228 aircraft (see Tab. 1).

[2] HABITALP – Alpine Habitat Diversity Project. INTERREG III B Alpenraumprogramm 2002-2006, http://habitalp.de, (last accessed on 20.03.2013)

Tab. 1: Instrument specifications (from http://apex-esa.org, last accessed 20.03.2013)

Spectral Range	VNIR: 380 - 970 nm SWIR: 940 - 2500 nm
Spectral Sampling Interval	VNIR: 0.55 - 8 nm over spectral range (unbinned) SWIR: 5 - 10 nm over spectral range
Spectral Resolution (FWHM)	VNIR: 0.6 - 6.3 nm over spectral range (unbinned) SWIR: 6.2 - 11 nm over spectral range
Spectral Bands	VNIR: default 114 bands, reprogrammable through customized binning pattern SWIR 199 bands
Spatial Pixels	1000
FOV (across track)	28°
IFOV	0.48 mrad
Spatial Sampling Interval (across track)	1.75 m @ 3500 m AGL (2 - 5 m at flight altitudes of 4 - 10 km)
Sensor dynamic range	VNIR: CCD, 14 bit encoding SWIR CMOS, 13 bit encoding
Pixel size	VNIR: 22.5 µm x 22.5 µm SWIR: 30 µm x 30 µm
Smile (average over FOV)	0.35 pixels
Keystone (frown, average over FOV)	0.35 pixels
Co-Registration (average over FOV)	0.6 pixels
Signal-to-Noise	SNR for various applications are available upon request Highest signal to noise ratio through advanced detector technology and pressure / temperature stabilization

3.3 Field data collection

Fieldwork was carried out to collect ground-truth data of the grassland. Twenty-five plots had previously been defined, which were distributed over the valley and at various altitudinal gradients in order to account for differences in species composition, productivity, phenological stages and soil type. A map with the sample plots indicated is shown in Fig. 2.

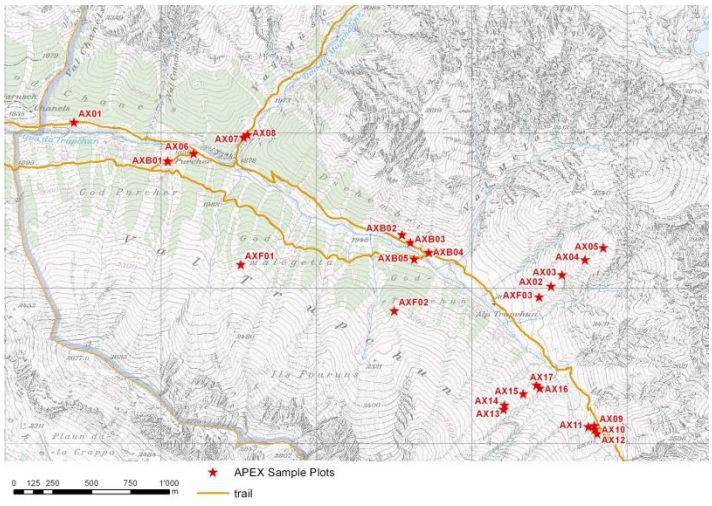

Fig. 2: Locations of the 25 sample plots in Val Trupchun, where 1x1 m of vegetation was clipped.

The plots were chosen at locations with vegetation as homogenous as possible, and squares of 6 x 6 m were marked. The corners of the plots were marked with flags and measured with a differential global positioning system (GPS), device type Leica RX 1210 T. On 24 of June 2010, on the same day as the flight, above-ground biomass was clipped within a $1m^2$ subplot located in the middle of each plot. The vegetation samples were sealed in plastic bags and weighed the same day in order to determine wet biomass. Afterwards, the samples were dried in the oven at 65° for 48 hours and weighed again to determine dry biomass.

3.4 Image acquisition and pre-processing

The APEX flight was carried out on 24 of June under cloud free conditions. The specific study site Val Trupchun was covered by four image strips, each with an extend of about 2x6 km and a ground resolution of 2 m. The flight lines are SW to NE oriented, cross-wise to the valley and the mountain ridge. The image strips were atmospherically and geometrically corrected by RSL using standard procedures. The atmospheric correction was computed using the ACTOR-4 software tool to obtain hemispherical-conical-reflectance (HCRF) data (Schläpfer & Richter 2002). The geometrical correction was made using the Parametric Geocorrection (PARGE) software (Schläpfer & Richter, 2002). The geometric distortions of the orthorectified data were evaluated based on ground based GPS measurements and were found to be less than one pixel (+/- 2m) (Damm et al., 2012). However, there were differences between the reflectance of similar pixels in the overlapping regions between image strips due to different view angles and effects of surface anisotropy (Weyermann et al., 2013).

3.5 Data analysis

To extract APEX reflectance data at the sample locations, the following procedure was applied: A square of 6x6 m around the centre coordinate of the plots was imported into the ENVI 4.7 software. This square corresponded to 9 pixels (3x3 pixels) of the APEX data from which the average reflectance was extracted as reference value. There were plots lying on more than one strip because of the overlapping zone, so that two reference reflectance values were available for one sample. These values were considered as independent measurement points. Consequently, there were 43 measurement points available, from which 18 points were double (same ground truth biomass value, but different reference reflectance).

The biomass samples were divided into two groups, one used for the calibration (22 points), and one for the validation (21 points) of the model using a stratified random sampling approach. An empirical

$$NDVI = \frac{NIR - RED}{NIR + RED} = \frac{R_{808.8} - R_{664.3}}{R_{808.8} + R_{664.3}}$$

model was developed based on the 22 calibration samples. The standard NDVI was calculated based on band 50 (664.3 nm) and band 86 (808.8 nm) by using the following formula:

where R is the reflectance at the specific wavelength.

The calculated NDVI was regressed against the calibration biomass samples in an exponential regression to obtain the coefficient of determination (R^2) for calibration. An exponential (instead of linear) regression can be implemented due to the large volume scattering of vegetation that induces sensor saturation at high densities.

Since APEX provides more bands in the red (600 - 700 nm) and NIR (700 - 1300 nm), we tested if calibration results could be improved by calculating simple ratio vegetation indices (SRI) with all possible combinations of 301 bands and regressing them against the calibration data set.

$$SRI = \frac{R_a}{R_b}$$

where R_a and R_b is the reflectance at wavelength a and b, respectively.

Spearman's rank correlation coefficients (R) resulting from the regression analysis were plotted on a 2D-contour plot to evaluate R characteristic patterns and identify the best wavelength combination. This procedure allowed the selection of optimal bands to be used in the calculation of the index. Band combinations with maximized correlation with biomass were chosen, considering cause effect relationships between spectral bands and underlying absorption and scattering processes. For the final model we chose the best SRI within the range of the visible (RED) for the first band and near-infrared (NIR) (700 - 1300 nm) region for the second band. Within this range, high reflection occurs on healthy biomass, and no water absorption interferes with the signal. With the chosen SRI we computed an exponential regression model to predict and map biomass content.

For all correlations between biomass sample and APEX reflectance spectra, the comparison was carried out using the wet weight of the biomass samples. Predictive performance of the biomass model was computed with the independent validation data set. The coefficient of determination (R^2) and the root mean square error (RMSE) were calculated to compare the predicted with the observed values.

The biomass prediction model is only valid for grassland. A linear spectral unmixing method (LSU) was performed to separate different land cover classes and to extract the grassland. LSU is a classification approach that can be used for hyperspectral imagery based on the materials' spectral characteristics. The reflectance at each pixel of the image is assumed to be a linear combination of the reflectance of each material present within the pixel (Boardman, 1989). The measured spectrum of a mixed pixel is decomposed into the set of corresponding fractions (endmembers) that indicate the proportion of each endmember present in the pixel. The linear unmixing method is assigning each pixel into the predefined classes based on the abundance values of each endmember.

4 RESULTS

4.1 Regression of biomass and standard NDVI

The standard NDVI was calculated using APEX band 50 and 86 located at 664.3 nm and 808.8 nm. A correlation with the calibration data set was computed, and an exponential regression yielded the best fit with an R^2 of 0.74, shown in Fig. 4.

The validation of the model was carried out by calculating the predicted biomass using the calibration model at the validation sample plots and comparing them against the true wet weight values. The R^2 and the RMSE were 0.54 and 236 g/m^2 respectively.

Plots AX06, AX07 and AX14 differ most from the prediction.

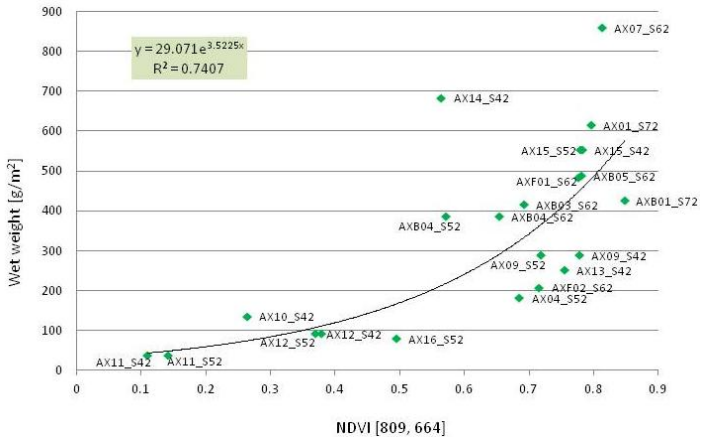

Fig. 3: Regression between the standard NDVI derived from APEX reflectance spectra from bands at 809 and 664 nm and the wet weight biomass calibration sample data

AX06 is located at Alp Purcher, next to a former alp hut, where tall-herb communities dominated by stinging nettle (*Urtica dioica*, L.) and monkshood (*Aconitum napellus ssp. Vulgare*, DC.) occur. The model predicts that there should be less biomass than the measured value. The biomass at AX14 and AX07 is also underestimated from the model. AX07 is situated at the entrance of Val Müschauns on a spot with ruderal vegetation.

It can be concluded that the model based on the standard NDVI generally underestimates biomass values above 600 g/m^2.

4.2 Regression of Biomass and Optimal Simple Ratio Index

To optimize the model, simple ratio indices (SRI) were calculated with all possible combinations of bands and correlated against the calibration data set. Spearman's rank correlation coefficients (R) were plotted on a 2D-contour plot to identify the best wavelength

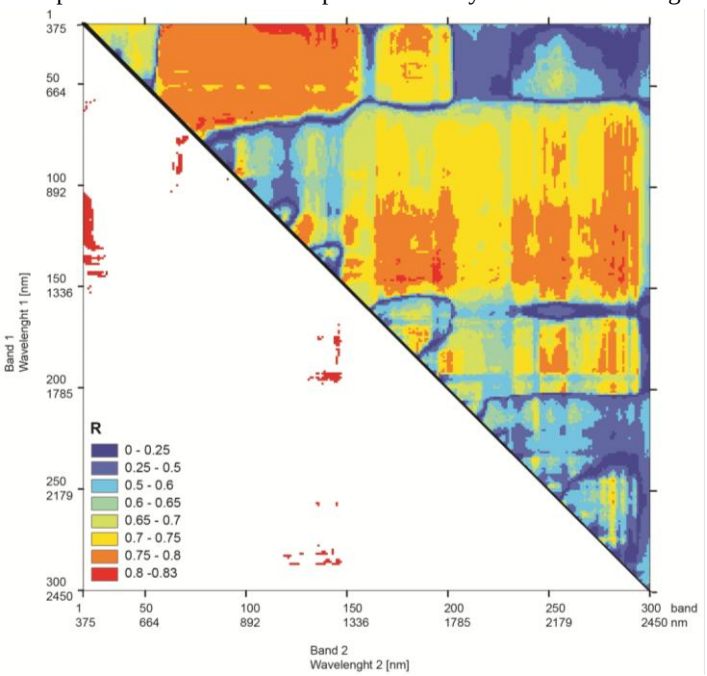

Fig. 4: 2D-correlation plot that shows the correlation coefficient R (Spearman's Rank) between SR indices and biomass. The matrix is symmetrical. Below the diagonal, band combinations are marked in red where R>0.8.

combination, shown in Fig. 4.

For our final biomass model the best SRI within the range of visible (RED) and near-infrared (NIR) (700 - 1300 nm) region was chosen. Within this range high reflection on healthy biomass occurred and no water absorption interfered with the signal.

The SRI of band 92 (842 nm) and band 68 (727 nm) achieved the best R (0.823) overall. This combination was chosen for the final biomass model. An exponential regression model was computed again between SRI and wet weight biomass of the calibration data set resulting in an R^2 of 0.77.

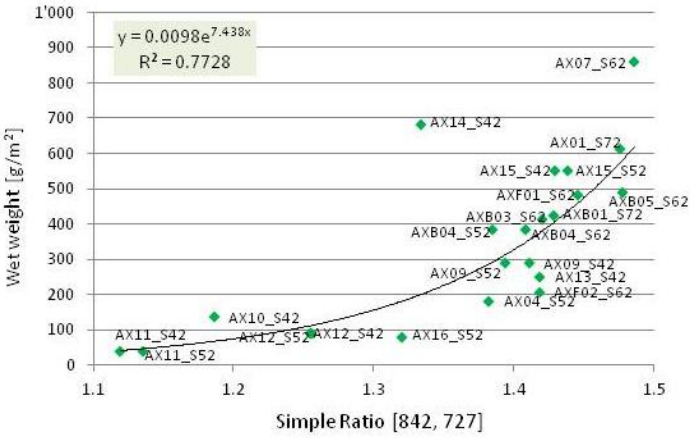

Fig. 5: Regression between SRI derived from APEX reflectance spectra from band at 842 nm and 727 nm and the wet weight biomass calibration sample data.

The validation of the model was carried out by calculating the predicted biomass using the model equation for the validation sample plots and comparing them to the true wet weight values. The R^2 and RMSE were 0.57 and 238 g/m^2 respectively.

Generally the pattern of the plots was comparable to the NDVI model. The outliers were again AX14, AX06 and AX07. The calibration model under-estimated biomass values above 600 g/m^2.

4.3 Regression of biomass and narrowband SRI

According to Mutanga and Skidmore (2004) a narrow band SRI, both located in the far RED (around 750 nm) should solve the saturation problem which means that sample locations with high biomass occurrence aren't underestimated.

To analyse this thesis, the best R around two bands in the far RED was selected from the 2D-correlation plot (cf. Fig. 4). The SRI between band at 765 nm and band at 735 nm has an R of 0.810 and is thus only slightly lower compared to the highest R (0.823) for the optimal SRI at bands 92 and 68. The model was recalculated with these two bands to check for a possible model improvement.

The coefficient of determination (R^2) is 0.7697, which is only slightly lower than our best SRI (R^2 = 0.7728). On the other hand, the validation yielded 10% better validity (67%). High biomass values were still underestimated, but at a lower level than with the best SRI model.

4.4 Biomass map

The best SRI regression model (band 842 and 727 nm) that was found for the estimation of biomass was applied to the APEX image. Only image pixels representing grassland were considered. The grassland was extracted by carrying out an LSU classification with the APEX data. Fig. 6 shows the resulting biomass prediction map.

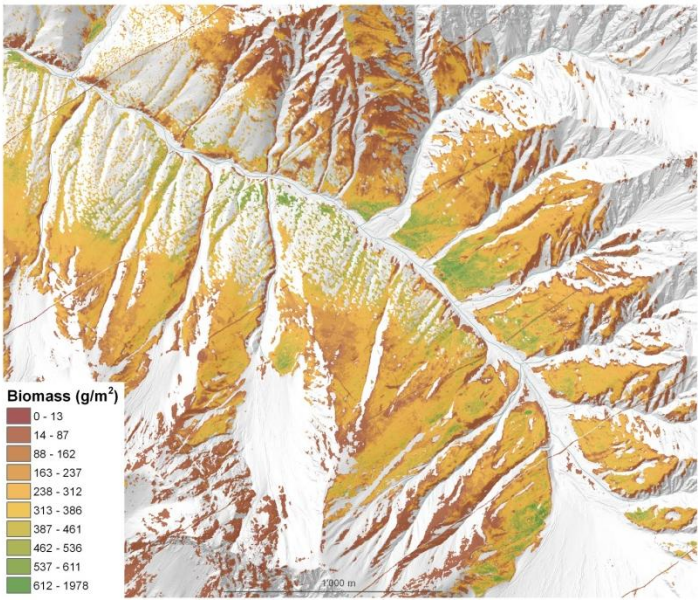

Fig. 6: Biomass map of Val Trupchun

Estimated biomass values were generally in a reasonable range. On the map, it can be seen that biomass decreases with increasing altitude at the slopes. Three locations with high biomass are noticeable. The highest biomass sources are located around the former Alp Trupchun. High sources are also visible around former Alp Purcher. Another spot with remarkably high occurrence is situated at the end of the valley on the bottom south slope. It can be concluded that high biomass concentration occurs where former anthropogenic activities took place (cattle or sheep excreta).

4.5 Variability of sample plot location

For the uncertainty analysis of our model an investigation of the sample plot location lying on more than one strip have been carried out. The differences of the SRI between the overlapping image strips were analysed by the variability of the plots located on two strips by a scatter plot, illustrated in Fig. 7.

The analysis is done for our optimal SRI with band 842 and 727 nm. The SRI value from one strip is plotted against the same SRI of the other strip for the double plots. The coefficient of determination R2 is acceptable with 0.96.

The quantification of these differences with respect to the biomass prediction produced a mean error of 12%.

5 Discussion

5.1 Comparision of NDVI and optimal SRI

NDVI and SR indices are functionally related (Liang, 2005), however SR indices are often used in mountainous regions (Boschetti et al., 2007) since they enhance the contrast between soil and vegetation, minimize the effects of the illumination conditions (Baret and Guyot, 1991) and reduce shadow effects (Boschetti et al., 2007). Additionally, the presented results indicate a better performance of the optimal SRI compared to the NDVI and an improved the predictive accuracy of the SRI for biomass. The coefficient of determination R^2 increased from 0.74 for the standard NDVI to 0.77 for the SRI model. The validation is also slightly improved from 0.54 to 0.56 (R^2). The quality of the model with an accuracy of 57% is good

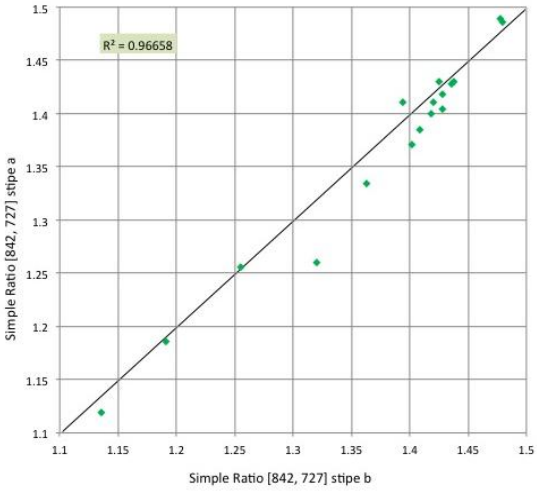

Fig. 7: Scatter plot of the optimal SRI values of all sample plots on APEX strip a against strip b

regarding the challenging terrain with slopes up to 78°. This means that 57% of the variation in biomass on an independent test data set could be explained by the model.

Both models are non-linear and underestimate high biomass values (above 600 g/m^2). Such bias can be caused by random noise or fundamentally non-linear relationship in the true physical relationship (Geladi et al., 1999). Another reason is saturation of NIR reflectance in dense vegetation, which frequently affects NDVI and slightly less SR indices. Broad bands for VIs, one in RED and one in NIR, have been shown to saturate at high biomass or high LAI (Mutanga & Skidmore, 2004). For our SRI we chose two closer bands (730 vs. 840 nm), still located in RED and NIR.

However, the saturation effect should only occur typically in multilayer vegetation such as forests or agricultural crops, with LAI > 4 (Baret & Guyot, 1991). The grassland of Val Trupchun would probably have a LAI around 3. Nevertheless, our SRI model still underestimates high biomass. Based on this fact the model was recalculated using two narrow bands, both located in the far RED, as this should solve the saturation problem according to Mutanga and Skidmore (2004). The coefficient of determination (R^2) between band 77 at 765 nm and band 70 at 735 nm is 0.7697, which is only slightly lower than our best SRI (R^2 = 0.7728). On the other hand, the validation yielded 10% better validity (67%). It can be concluded that high biomass values were still underestimated, but at a lower level when avoiding the NIR domain.

5.2 Uncertainty Analysis

The 57% accuracy of the SRI model (842/747) validation means that 57% of the biomass variance can be explained. This is a comparatively good validation for such a complex terrain conducted with completely independent plots. However, several factors showed that the model is relatively instable. The selection of the band combination is one important factor that influences the model accuracy, as illustrated by the example with the narrow band SR index (765/735) in the far RED. The best calibration should normally result in the best validation. Instead, we found a poorer calibration with a better validation result. This shows that our model alternates and that the sample size is not sufficient enough to develop a robust model. The sample size should be increased.

The selection of the calibration and validation data set also has an influence on the accuracy. Plots belonging to the calibration or the validation data sets have been chosen completely randomly. Tests with some manual settings, for example implementing the highest and the lowest biomass value into the calibration data set showed that the model output varied. We also tried dividing the double reference points from the different strips, assigning one to the calibration and the other to the validation data sets. However, these model adaptations didn't result in much improvement. The random selection for the calibration and validation data sets was justified and was therefore considered as the best solution. With this number of sample plots (n = 43), higher accuracies are almost impossible to reach. The uncertainties are mainly due to sensitivity to external factors, which overlap the measured signal and influence the model, such as atmospheric effects (cloud, haze and other scatterers), topographic effects (shading), illumination effects (sun angle and viewing geometry), soil effects (soil fraction), structural effects (scattering due to objects/leaf architecture) or random noise. Additionally, the sample itself also has some uncertainty derived from potential sampling inequality and weighting errors.

5.3 Different reflectance values between strips

The differences of the APEX data between the overlapping regions of the 4 strips are another point to be discussed. These differences are caused by the variations of illumination- viewing geometry in combination with surface anisotropy. Different parts of an image will view the surface at different angles, so that clear brightness gradients may often be detected across the image. In fact, the spectral signal reflected from surfaces such as plant canopies is determined by its intrinsic surface anisotropy and consequently varies as a function of the angle of view and the angle of illumination. Shadows are also influenced by different illumination angles. During the precalibration of the image, these effects are compensated to the best possible extent during the basic Bidirectional reflectance distribution function (BRDF) corrections. However, notable differences usually exist as long as no sophisticated BRDF corrections are applied. Therefore, the reflectance of the image pixel of a strip is slightly different from the reflectance of the same pixel available on the neighbouring strip.

We haven't computed any artificial reflectance averaging to obtain one value per image pixel for the overlapping regions. A possibility would have been to build a mosaic of all four strips implementing the reflectance average or favouring one strip. However, each manual computation also involves uncertainties and needs to be justified. It was also not possible to take a single reflectance value from one strip, since we did not record the exact clipping time of every plot. We therefore cannot tell which of the strips correspond better to the biomass data measured. Therefore we decided not to carry out such an artificial intervention with the APEX data and keep all original values from the two strips as independent data.

The scatter plot showed a coefficient of determination R^2 of 0.96 for our optimal SRI (842/727). The same analysis for the narrow band index (765/735) resulted an R^2 of 0.95. Several studies showed that using a narrow band combination in RED is less sensitive to varying soil brightness, atmospheric condition and sensor view angle compared to a broad band combination (Blackburn & Pitman, 1999). With this example this assumption can't be confirmed. Our band selection for the optimal SRI is evidently enough narrow to keep this effect small.

6 CONCLUSION

Imaging spectroscopy techniques permit not only the classification of vegetation, but also the quantitative mapping of different vegetation variables due to their high spectral and spatial resolution. This study demonstrates the utility of vegetation indices involving APEX bands for estimating biomass in alpine grasslands.

SRI and NDVI models were suitable for the modelling of biomass prediction maps implementing biophysical parameters. We found that the correlation between biomass *insitu* measurements and SRIs was non-linear, most likely due to sensor saturation. Our optimal SRI improved the model quality compared to a standard NDVI model. All computed models underestimated high biomass values above 600 g/m^2. The model accuracy of 57% was good considering the challenging terrain. However, several factors showed that the model was relatively unstable due to parameter input settings and external factors. Differences in APEX data between strips induced an important effect, due to different illumination/view angles. The quantification regarding biomass prediction due to these differences produced a mean error of 12% for the sample plots.

The biomass prediction map showed plausible values for the grassland with high concentrations around the former Alp Trupchun, Alp Purcher and on the south slope at the end of the valley. We found that high biomass sources were linked to former anthropogenic land use, dominant vegetation structure and to preferred ungulate habitat today.

The high-resolution map is now a useful basis for future research in the SNP to investigate forage amount and analyse ungulate habitat pattern in Val Trupchun.

7 OUTLOOK

The generated biomass prediction map can be used for future research in Val Trupchun. This work was carried out within the scope of a PhD thesis at the Swiss National Park analysing ungulate habitat patterns relating to biophysical and biochemical parameters. The APEX campaigns have been continued during the years 2011 and 2012.

The produced model is applicable only for the study area, since semi-empirical. These predictive models are site- and sensor-specific and unsuitable for application to other areas or to different seasons. With this model we tried to predict another area of the SNP, the grassland of Il Fuorn, which is located ca. 15 km north-east, and didn't find suitable agreement with *insitu* measurements. This finding highlights the importance of local models, based on local measurements for small scales in complex terrain.

Moreover, our model is only valid for the time of the image, which was June. To analyse temporal changes for biomass, the APEX campaign should be carried out several times a year.

The main proposal for a model improvement based on this work is to increase the number of sample plots in the study area. With more samples covering the full range of biomass concentrations, we suppose that the model accuracy and stability will improve. Another possibility would be to clip more than 1 m^2 per sample plot to get more than one sample out of one plot. Thus, small-scale variability could be improved, too. However, all improvement proposals would require a lot more effort in the field which is a limiting factor.

ACKNOWLEDGMENT

The author wishs to thank to Anna Schweiger, Alexander Damm, Mathias Kneubühler, Ruedi Haller, Pia Anderwald and Antonia Eisenhut.

REFERENCES

[1] Achermann, G., Schütz, M., Krüsi, B. O., 2000. Tall-herb communities in the Swiss National Park: Long-term development of the vegetation. Nationalpark-Forschung in der Schweiz, Band 89.

[2] Baret, F., Guyot, G., 1991. Potentials and limits of vegetation indices for LAI and APAR assessment. Remote Sensing of Environment, 35, pp. 161-173.

[3] Beeri, O., Phillips, R., Hendrickson, J., Frank, A. B., Kronberg, S., 2007. Estimating forage quantity and quality using aerial hyperspectral imagery for northern mixed-grass prairie. Remote Sensing of Environment, 110, pp. 216-225.

[4] Birth, G. S., McVey, G. R., 1968. Measuring the colour of growing turf with a reflectance spectrophotometer. Agronomy Journal 60, pp 640-643.

[5] Blackburn, G. A., Pitman, J. I., 1999. Biophysical controls on the directional spectral reflectance properties of bracken (Pteridium aquilinum) canopies: results of a field experiment. International Journal of Remote Sensing, 20(11), pp. 2265-2282.

[6] Boardman, J. W., 1989. Inversion of imaging spectrometry data using singular value decomposition: Proceedings, IGARSS'89, 12th Canadian Symposium on Remote Sensing 4, pp. 2069-2072.

[7] Boschetti, M., Bocchi, S., Brivio, P. A., 2007. Assessment of pasture production in the Italian Alps using spectrometric and remote sensing information. Agriculture, Ecosystems Environment, 118(1-4), pp. 267-272.

[8] Braun-Blanquet, J., Brunies, S., Campell, K., Frey, E., Jenny, H., Meylan, Cli. & Pallmann, H., 1931. Vegetationsentwicklung im Schweiz. Nationalpark. Ergebnisse der Untersuchung von Dauerbeobachtungsflächen, 1. Dokumente zur Untersuchung des Schweizer Nationalparks. Jahresberichte der Nationalforschenden Gesellschaft Graubündens, 69, pp. 3-82.

[9] Braun-Blanquet, J., Pallmann, H., Bach, R., 1954. Planzensoziologische und bodenkundliche Untersuchungen im Schweizerischen Nationalpark und seinen Nachbargebieten. II Vegetation und Böden der Wald- und Zwergstrauchgesellschaften (Vaccinio-Piceetalia). Ergebnisse der wissenschaftlichen Untersuchungen des schweizerischen Nationalparks. Band 4, Kapitel 28.

[10] Cho, M. A., Skidmore, A., Corsi, F., van Wieren, S. E., Sobhan, I., 2007. Estimation of green grass/herb biomass from airborne hyperspectral imagery using spectral indices and partial least squares regression. International Journal of Applied Earth Observation and Geoinformation 9, pp. 414-424.

[11] Damm, A., Kneubühler, M., Schaepman, M. E., Rascher, U., 2012. Evaluation of gross primary production (GPP) variability over several ecosystems in Switzerland using sun-induced chlorophyll fluorescence derived from APEX data. Proc, IGARSS 2012, Munich (D), July 22-27 2012, pp. 7133-7136.

[12] Geladi, P., Hadjiiski, L., Hopke, P., 1999. Multiple regression for environmental data: nonlinearities and prediction bias. Chemometrics Intell. Lab. Syst. 47 (2), pp 165-173.

[13] He, Y., Guo, X.L., Wilmshurst, J., 2006. Studying mixed grassland ecosystems I: suitable hyperspectral vegetation indices. Canadian Journal of Remote Sensing 32, pp. 98-107.

[14] Liang, S., 2004. Quantitative remote sensing of land surfaces. Hoboken: Wiley, Hoboken.

[15] Mirik, M., Norland, J. E., Crabtree, R. L., Biondini, M. E., 2005b. Hyperspectral one-meter-resolution remote sensing in Yellowstone National Park,

Wyoming: II. Biomass. Rangeland Ecology and Management 58, pp. 459-465.

[16] Mutanga, O., Skidmore, A. K., 2004. Narrow band vegetation indices overcome the saturation problem in biomass estimation. International Journal of Remote Sensing, Vol. 25, pp. 3999-4014.

[17] Mutanga, O., Skidmore, A. K., 2007. Red edge shift and biochemical content in grass canopies. ISPRS Journal of Photogrammetry and Remote Sensing 62, pp. 34-42.

[18] Mutanga, O., Skidmore, A. K., Prins, H. H. T., 2004. Predicting in situ pasture quality in the Kruger National Park, South Africa, using continuum-removed absorption features. Remote Sensing of Environment, 89, pp. 393-408.

[19] Numata, I., Roberts, D. A., Chadwick, O. A., Schimel, J., Sampaio, F. R., Leonidas, F. C., Soares, J. V., 2007. Characterization of pasture biophysical properties and the impact of grazing intensity using remotely sensed data. Remote Sensing of Environment, 109, pp. 314-327.

[20] Parolini, J. D., 1995. Zur Geschichte der Waldnutzung im Gebiet des Schweizerischen Nationalparks. PhD Thesis ETH Zurich, Nr. 1187.

[21] Psomas, A., 2009. Hyperspectral remote sensing for ecological analyses of grasslands ecosystems. Spectral separability and derivation of NPP related biophysical and biochemical parameters. Dissertation, University of Zurich.

[22] Rahman A. F., Gamon J. A., 2004. Detecting biophysical properties of a semi-arid grassland and distinguishing burned from unburned areas with hyperspectral reflectance. Journal of Arid Environments 58(4), pp. 597-610.

[23] Rouse, J. W., Haas, R. H., Schell, J. A., Deering, D. W., Harlan, J C., 1974. Monitoring the vernal advancement and retrogradation (greenwave effect) of natural vegetation. NASA/GSFC Final report, Greenbelt, MD, USA.

[24] Schläpfer, D., Richter, R., 2002. Geo-atmospheric processing of airborne imaging spectrometry data. Part 1: parametric orthorectification. International Journal of Remote Sensing, Vol. 23, pp. 2609-2630.

[25] Tarr, A. B., Moore, K. J., Dixon, P. M., 2005. Spectral reflectance as a covariate for estimating pasture productivity and composition. Crop Science, 45(3), pp. 996-1003.

[26] Trepp, W., Campell, E., 1968. Vegetationskarte des Schweizerischen Nationalpark. Nationalparkforschung in der Schweiz, Band 11, Heft 58

[27] Tucker, C. J., 1979. Red and photographic infrared linear combinations for monitoring vegetation. Remote Sensing of Environment 8, pp 127-150.

[28] Zoller, H., 1992. Vegetationskarte des Schweizerischen Nationalparks und seiner Umgebung. Nationalpark-Forschung in der Schweiz, Band 85.